ELSEVIER

Journal of Nuclear Materials 307–311 (2002) 971–975

journal of nuclear materials

www.elsevier.com/locate/jnucmat

Phase transformation in the γ-TiAl alloy induced by Ar ions

M. Song *, K. Mitsuishi, M. Takeguchi, K. Furuya, T. Tanabe, T. Noda

National Institute for Materials Science, Nano-Materials Laboratory, 3-13 Sakura, Tsukuba 305-0003, Ibaraki, Japan

Abstract

Intermetallic γ-TiAl alloy specimens were irradiated with 25 keV Ar ions at room temperature. The defect formation and structural changes were investigated by conventional and high-resolution transmission electron microscopy. The defects observed in low-dose irradiated specimens are planar defects, which may be stacking faults or dislocation loops. A phase transformation was induced in high-dose irradiated specimens. The results suggest that the induced phase has a relation with the planar defects in the early stage of the ion irradiation. The induced phase was found to be of the same structure as the induced phase in Xe-irradiated γ-TiAl. The features of the ion irradiation induced structure changes are compared with reported results. The mechanism of the phase transformation is discussed.

1. Introduction

The changes of structure and properties of materials under energetic particle irradiation have been extensively investigated because of their importance to the design and application of the materials. Intermetallic TiAl alloys are used in airplane and spaceship manufacturing because of their high strength-to-weight ratio and good resistance under temperature variation conditions [1,2]. Potential applications of the material in other fields considered as a candidate for first wall materials of fusion reactors [3,4] are under research. Irradiations of the TiAl alloy with energetic particles have been studied by several groups. Dislocation loops and He bubbles were reported to be induced in TiAl alloys irradiated with electrons or He ions between 623 and 773 K [4–7]. Planar defects and rotated domains were observed in γ-TiAl alloys after He ion irradiation at room temperature [8,9]. Recently, the authors reported that a phase transformation was induced in γ-TiAl alloys with 50 keV Xe ion irradiation [10]. The phase transformation was considered to relate closely to the irradiation damages in the alloy introduced by the incident ions.

In the present work, the γ-TiAl specimens were irradiated with 25 keV Ar ions. The structure change in the specimens was investigated and compared with the results in Xe irradiated specimens. The mechanisms of the ion irradiation induced phase transformation are discussed.

2. Experimental

Single-phase γ-TiAl, with the compositions (wt%) of 36.8 Al(50.81 at.%), 0.038 O, 0.005 C, and Ti balanced, was used. Disks, 3 mm in diameter and 0.2 mm in thickness, were prepared mechanically and annealed at 1273 K for 1 h. The thin foil specimens were electropolished by a twin jet technique in a solution of 10% perchloric acid and 90% ethanol at about 255 K.

Ion irradiations were carried out at room temperature in a system consisting of a 1000 kV high-voltage transmission electron microscope (HVTEM, JEM-ARM1000), and 200 and 30 kV ion implanters [11]. The energy of the Ar ions was 25 keV. The stopping range of the ions calculated with the TRIM code [12] was about 25 nm in γ-TiAl. Therefore, the implanted ions were estimated to stop in the thin area of the specimens appropriate for observation by conventional and high-resolution transmission electron microscopy (CTEM and HRTEM). The electron beam was switched off

* Corresponding author. Tel./fax: +81-298 59 5054.
E-mail address: minghui.song@nims.go.jp (M. Song).

0022-3115/02/$ - see front matter
PII: S0022-3115(02)00984-4

during ion implantation. The maximum dose of Ar ions was 1.1×10^{20} ions m^{-2}. The specimens were observed using the HVTEM operated at 1000 kV.

3. Results and discussions

Fig. 1 shows micrographs and the corresponding selected area diffraction (SAD) patterns of a specimen before and after the irradiation. The grain size of the γ-TiAl is of the order of micrometers, so that usually a single-crystal grain is observed with the TEM. Fig. 1(a) is a bright-field (BF) TEM image before irradiation, in which crystal defects can almost not be found. At an irradiation dose of about 2.2×10^{19} ions m^{-2}, planar defects with a size of about 10 nm in length are seen. A and B in Fig. 1(c) indicate two orientation variants of the defects. Each of them has their long side parallel to one of the edge-on {1 1 1} planes of the matrix. In the SAD pattern of Fig. 1(d), streaks along ⟨1 1 1⟩ directions and cross-sectioned with diffraction spots are seen. These streaks are considered to be reflected from the planar defects similar to the A and B defects in Fig. 1(c), since they have a small size in ⟨1 1 1⟩ direction. The planar defects and the streaks in the SAD pattern were also observed in He irradiated γ-TiAl [8,9]. At an irradiation dose of 1.1×10^{20} ions m^{-2}, irradiation defects showed a quite different morphology as illustrated in Fig. 1(e). The defects have a size of 10–20 nm in width and several ten nanometers in length. Similar to the planar defects in Fig. 1(c), the defects have two variants and each of them parallel to one of the {1 1 1} plane of γ-TiAl, but they have a width and have fringes on them. The morphology of these defects is similar to the Xe-induced phase [10], but in relatively smaller size. Extra spots are also observed in the corresponding SAD pattern as shown by E, F, G and H in Fig. 1(f). Though these extra spots are not as apparent as those in Xe-irradiated γ-TiAl specimens, they are exactly in the same position in the SAD patterns as those observed in the SAD patterns of Xe-irradiated γ-TiAl specimens. These results indicate that phase transformation similar to that in Xe-irradiated γ-TiAl specimens is also induced in the Ar-irradiated specimens.

Fig. 2 shows a set of BF and dark-field (DF) images and the SAD pattern of a specimen irradiated with Ar ions to a dose of 1.1×10^{20} ions m^{-2}. The induced phase regions indicated by A and B are seen in Fig. 2(a) with sizes of several tens of nanometer. The DF image in Fig. 2(c) was obtained using the extra spot C in Fig. 2(b). The induced phase region A appears bright. This fact indicates that the regions with their long sides parallel to $(1\,\bar{1}\,1)$ contribute to the extra spot C. The DF image of Fig. 2(d) was obtained using the extra spot D in Fig. 2(b). The region B looks bright while A looks dark. These results reveal that regions A and B belong to different variants, which are independent of each other. The extra spots C and D correspond to the two transformed phase variants, respectively.

Fig. 3 is a HRTEM micrograph of a specimen irradiated with Ar ions to a dose of 1.1×10^{20} ions m^{-2}. Induced phase regions are indicated by P. The matrix

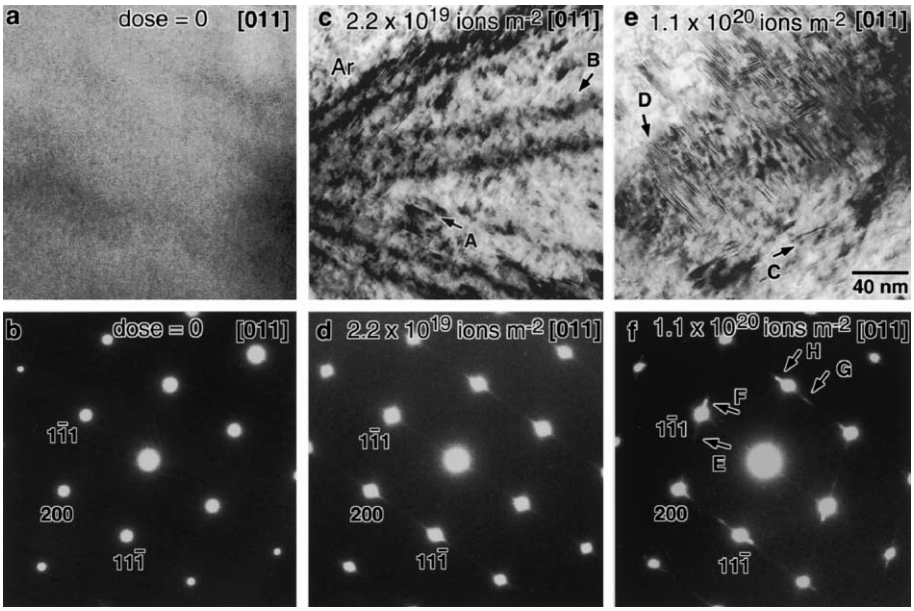

Fig. 1. TEM BF images and SAD patterns of a γ-TiAl specimen irradiated with 25 keV Ar ions at room temperature. (a) and (b) before irradiation; (c) and (d) at a dose 2.2×10^{19} ions m^{-2}; (e) and (f) at a dose 1.1×10^{20} ions m^{-2}.

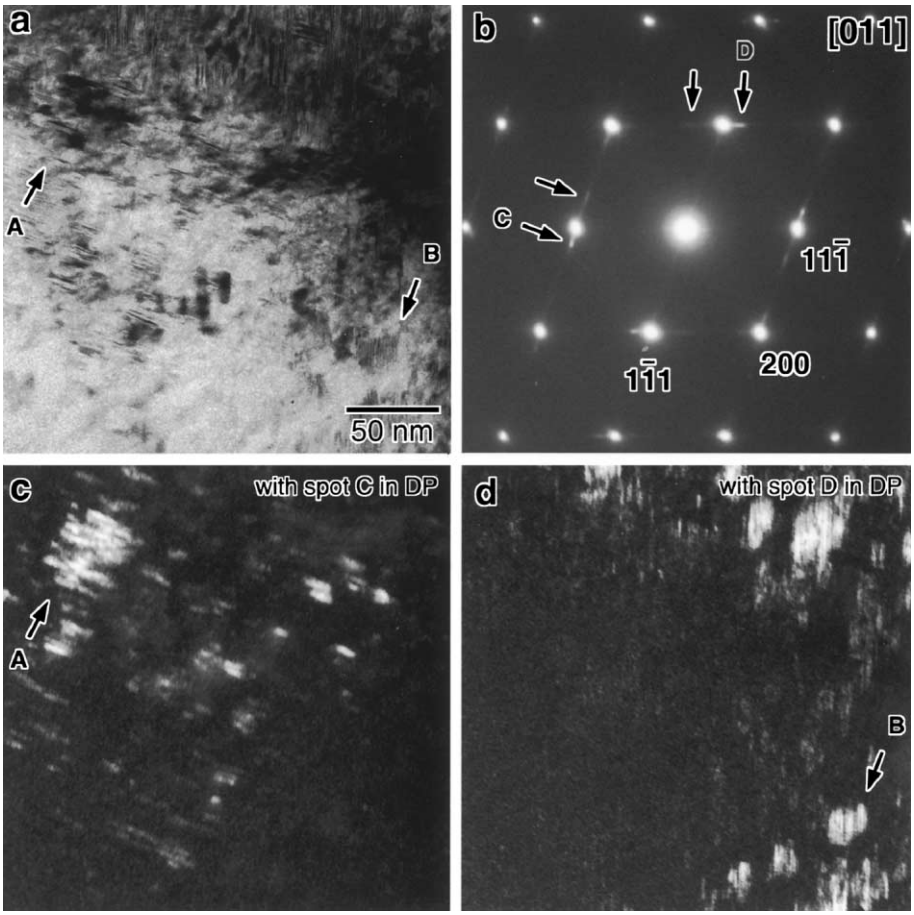

Fig. 2. TEM BF and DF images and an SAD pattern of a γ-TiAl specimen irradiated with 25 keV Ar ions to a dose 1.1×10^{20} ions m^{-2} at room temperature. (a) A BF image; (b) the corresponding SAD pattern; (c) a DF image with spot C in (b); (d) a DF image with spot D in (b).

indicated by M surrounds the regions. Arrows A and B indicate the interface of the region and the matrix. It is obvious that the phase region has a coherent and relatively flat interface with the matrix along $(1\,1\,\bar{1})$ as indicated by arrows A, and zig-zag interfaces along other lattice planes. These facts suggest that the phase-transformed region grows easier along interfaces other than $\{1\,1\,1\}$. It is probably the reason why the typical shape of an induced phase region is narrow along $\langle 1\,1\,1\rangle$ as observed in Figs. 1 and 2. The abcabc in region M and ababab in region P in Fig. 3 show the stacking sequences of the most-dense atomic lattice faces in two regions, respectively. It is known from the stacking sequence of the lattice planes that the induced phase is of an hcp structure, the same as that of the Xe induced phase [10]. The orientation relationships of the induced phase with the matrix are also the same as those of the Xe induced phase, namely, $(0\,0\,1)_P \| (1\,1\,1)_\gamma$ and $[1\,0\,0]_P \| [0\,1\,1]_\gamma$. The crystal parameters of this phase are calculated based on the measurements from both HRTEM images and SAD patterns as $a = 0.28(6)$ nm, $c = 0.46(2)$ nm. They have the same parameters as those of the induced phase in Xe-irradiated γ-TiAl specimens [10].

The present work reveals that the irradiation with 25 keV Ar also induces a phase transformation in the γ-TiAl alloy, but the dose at which the induced phase can be observed is much higher than the dose of Xe ions in Xe-irradiation experiments. For Ar, the dose is about 1.1×10^{20} ions m^{-2}, while the dose is about 2.2×10^{18} ions m^{-2} for Xe [10]. The displacements per atom (dpa) and the average content of irradiated ions in the damage region of the irradiated specimens were calculated with TRIM code. At the above dose for Ar, the dpa of the irradiated specimen are 15.9, the average content of Ar in the damage region is 42.45 at. ppm, whereas at the above dose for Xe, the dpa of the irradiated specimen is 2.49, and the Xe content is 2.97 at. ppm. Both the dpa and atomic content of Ar atoms in Ar-irradiated

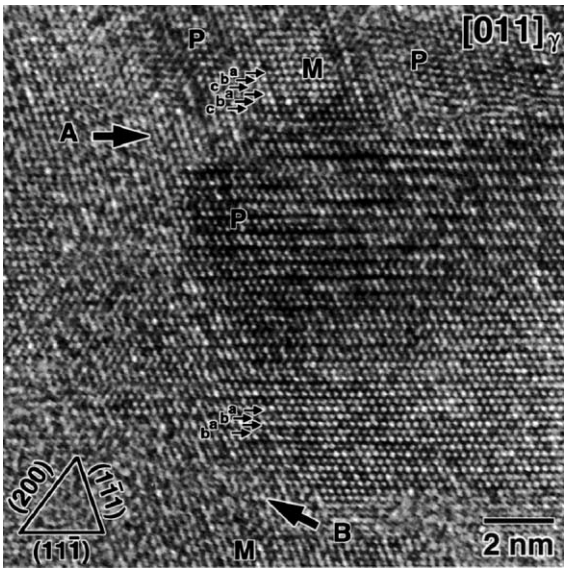

Fig. 3. An HRTEM micrograph of γ-TiAl specimen irradiated with 25 keV Ar ions to a dose 1.1×10^{20} ions m^{-2} at room temperature. P and M indicate the induced phase and matrix respectively.

specimens are much higher than the dpa and content of Xe atoms in Xe-irradiated specimens, but the induced phase in Ar irradiated specimens at the above Ar dose is not as much as that in Xe-irradiated specimens at the above Xe dose [10]. The results confirmed that the dpa and implanted ion content are not enough to characterize the structure changes, especially the phase transformation in γ-TiAl.

It is known that one of the damage effects of ion irradiation to a material is the formation of point defects. These defects are directly related to the dpa in the materials. Gathered point defects may form dislocation loops. Diffusion of the point defects may increase the size of dislocation loops or form stacking faults (SFs). This case is true for Xe, Ar and He ion irradiations, for electron irradiation, or for other energetic particle irradiations. This process may usually not change the local composition because a displaced atom leaves its vacancies in only several atomic lattice distances [13]. For γ-TiAl, these dislocation loops or SFs may not become an induced phase if the composition of the local area does not change, since the ordered γ-TiAl phase is a stable phase up to its melting point. Energy dispersive X-ray spectroscopy analysis revealed that the Xe content in the Xe-induced phase in γ-TiAl is 1.5 times higher than in the γ-TiAl matrix [10]. Considering this fact, we suppose that the composition change in a local region is relevant to the phase transformation. Though the difference of composition between the Ar-induced phase and the γ-TiAl matrix is not known yet, we suppose that there exists similar tendency of Ar gathering in Ar-induced phase as to Xe in Xe-induced phase. An incident ion may collide with atoms in the irradiated γ-TiAl matrix and may displace atoms cascadely especially around the stopping region. If the dpa in the cascade process are large enough, the matrix may becomes a liquid-like arrangement, so called a 'thermal spike' [13]. The composition change may occur during the thermal spike forming and cooling. In a thermal spike, there may exist a high vacancy concentration and a high fluid state for atoms to move easily. Since the inert gas atoms do not solve in crystalline γ-TiAl, they have a tendency to move towards the region of the spike. This may be the reason why the content of Xe in the induced phase is much higher than in the matrix. When the high-Xe included phase solidifies, the γ-TiAl phase may not be favorable in energy while the hcp phase is favorable in energy. So the hcp phase nucleates and grows larger during the subsequent irradiation. The mass of a Xe ion (131 atomic weights) is much larger than that of an Ar ion (40 atomic weights), therefore, the displacements per each incident ion of a Xe ion (970) is much larger than that of an Ar ion (340), calculated with TRIM code. So that an incident Xe ion may have a much heavier cascade than an Ar ion. This may be the reason why the phase transformation in the Ar-irradiated specimens is observed at much larger dpa and at-ppm than the Xe-irradiated specimens.

Two kinds of structure changes are observed in the present work. One is the formation of planar defects which are considered to be dislocation loops or SFs, and another is the induced phase transformation. The present work reveals that there are close relations between the two kinds of structural changes. These details need to be further investigated.

4. Conclusions

Intermetallic γ-TiAl alloy specimens were irradiated with 25 keV Ar ions at room temperature. The defect formation and the structural changes were investigated by CTEM and HRTEM. The defects observed in low-dose irradiated specimens are planar defects, which may be stacking faults or dislocation loops. In high-dose irradiated specimens, the phase transformation was induced. The results suggest that the induced phase has a relation with the planar defects in the early stage of ion irradiation. The induced phase was found to be in the same structure as that of the induced phase in Xe-irradiated γ-TiAl. The results indicate that the dpa and implanted ion content are not enough to characterize the structural change, especially the phase transformation in γ-TiAl. Thermal spikes formed during ion irradiation may relate to the composition change and the phase transformation.

References

[1] M. Matsuo, Iron Steel Inst. Japan Int. 31 (1991) 1212.
[2] F. Appel, R. Wagner, Mater. Sci. Eng. R22 (1998) 187.
[3] S. Mori, H. Miura, S. Yamazaki, T. Suzuki, A. Shimizu, Y. Seki, T. Kunugi, S. Nishino, N. Fujisawa, A. Hishinuma, M. Kikuchi, Fusion Technol. 21 (1992) 1744.
[4] A. Hishinuma, J. Nucl. Mater. 239 (1996) 267.
[5] K. Nakata, K. Fukai, A. Hishinuma, K. Ameyama, M. Tokizane, J. Nucl. Mater. 202 (1993) 39.
[6] K. Nakata, K. Fukai, A. Hishinuma, K. Ameyama, J. Nucl. Mater. 240 (1997) 221.
[7] A. Hishinuma, K. Nakata, K. Fukai, K. Ameyama, M. Tokizane, J. Nucl. Mater. 199 (1993) 167.
[8] M. Song, K. Furuya, T. Tanabe, T. Noda, J. Nucl. Mater. 271&272 (1999) 200.
[9] M. Song, K. Furuya, T. Tanabe, T. Noda, J. Electr. Microsc. 48 (1999) 355.
[10] M. Song, K. Furuya, T. Tanabe, T. Noda, Philos. Mag. Lett. 80 (2000) 661.
[11] K. Furuya, M. Piao, N. Ishikawa, T. Saito, Mater. Res. Soc. Symp. Proc. 439 (1997) 331.
[12] J.F. Ziegler, J.P. Biersack, U. Littmark, in: J.F. Ziegler (Ed.), The Stopping and Range of Ions in Solids, Pergamon, New York, 1985.
[13] W. Schilling, H. Ullmaier, in: R.W. Cahn, P. Haasen, E.J. Kramer (Eds.), Materials Science and Technology, Nuclear Materials, vol. 10B, VCH, Weinheim, 1994, p. 197.